Orientation-dependent morphological stability of grain boundary groove*

Wang Li-Lin(王理林)[a)b)], Lin Xin(林 鑫)[b)†], Wang Zhi-Jun(王志军)[b)], and Huang Wei-Dong(黄卫东)[b)]

[a)] School of Mechanical Engineering, Northwestern Polytechnical University, Xi'an 710072, China
[b)] State Key Laboratory of Solidification Processing, Northwestern Polytechnical University, Xi'an 710072, China

(Received 14 April 2014; revised manuscript received 19 May 2014; published online 10 October 2014)

Crystal orientation influences the morphological stability of solid–liquid interface during directional solidification of alloy, resulting in the variation of solidified microstructure. In this paper, the morphological evolution near grain boundary grooves (GBGs) with different crystal orientations in a dilute succinonitrile alloy under low temperature gradient and interface velocity is observed *in situ*. Under experimental conditions, the macroscopic solid–liquid interface is planar and keeps stable, while in GBGs there emerge protrusion and undulation. It is found that the morphological stability of GBG is dependent on crystal orientation. Specifically, for succinonitrile with a body-centered cubic crystal structure, GBGs around the ⟨100⟩ crystal orientation keep stable, while those apart from the ⟨100⟩ crystal orientation become unstable under the same conditions. So it is concluded that ⟨100⟩ crystal orientation favors the morphological stability of GBG.

Keywords: morphological instability, grain boundaries, crystal orientation, solidification

PACS: 47.20.Hw, 61.72.Mm, 81.10.Aj, 81.30.Fb **DOI:** 10.1088/1674-1056/23/12/124702

1. Introduction

Morphological evolution of solid–liquid interface during solidification determines the microstructure and thus performances of material. The morphological instability of planar interface in directional solidification was explained well using the linear stability analysis by Mullins and Sekerka.[1] Existence of GBGs along solid–liquid interface significantly influences the morphological stability. Coriell and Sekerka discussed the morphological stability near a GBG under directional solidification in a pure substance[2] and a binary alloy[3] through linear stability analysis. The results indicate that although the existence of a GBG does not change the stability–instability criterion, it provides an effective initial perturbation triggering the morphological instability of entire planar solid–liquid interface. Recently, phase field simulation of morphological instability near a GBG during directional solidification in a binary alloy was carried out by Yeh *et al*.[4] It is seen that the solute diffusion into the GBG results in the hump formation and the later morphological waves triggering the morphological instability.

Schaefer and Glicksman[5] made first attempt to observe the interface evolution near grain boundaries during directional solidification in a dilute succinonitrile alloy. They found that the interface near grain boundaries first becomes unstable and then forms parallel ridges to initiate dendritic growth. Noël *et al*.[6] also investigated experimentally the influence of grain boundaries on morphological instability during directional solidification of a dilute succinonitrile alloy in a cylindrical crucible. These studies have made great contributions to understanding the morphological evolution of a GBG under directional solidification.

In solidification, the solid–liquid interface properties are crystal-orientation-dependent. The interfacial energy anisotropy has been proved to influence morphological stability of a planar interface in theoretical analysis,[7–9] phase-field simulation[10,11] and experimental studies,[12,13] and subsequent dendritic growth[14,15] during directional solidification. It suggests that the interaction between anisotropic interface properties and solute diffusion ahead of the interface brings orientation-dependent solid–liquid interface stability. Considering the fact that the curved solid–liquid interface along GBG includes continuous crystal orientations, there should appear the crystal-orientation-dependent phenomena along the GBG.

In this paper, the morphology evolution of GBGs with different crystal orientations during directional solidification in a dilute succinonitrile alloy is continuously and *in situ* observed with an optical microscope. Then the effect of crystal orientation on groove interface stability is characterized.

2. Experimental apparatus and procedure

The sample used in our experiment was a dilute succinonitrile alloy, which has been universally accepted as a typical transparent model alloy for metal and widely used in solidification researches. The succinonitrile alloy was filled into a

*Project supported by the National Natural Science Foundation of China (Grant No. 51271213), the National Basic Research Program of China (Grant No. 2011CB610402), China Postdoctoral Science Foundation (Grant No. 2013M542384), and the Specialized Research Fund for the Doctoral Program of Higher Education of China (Grant No. 20116102110016).

†Corresponding author. E-mail: xlin@nwpu.edu.cn

© 2014 Chinese Physical Society and IOP Publishing Ltd

thin sandwiched sample cell under vacuum. The sample cell was made of two 50 mm×32 mm×0.17 mm glass plates glued together by epoxy resin adhesive. The inner thickness of sample was 120 μm. Three crystal grains were chosen in the sample cell. The middle grain's grooves were the research objects for studying the effect of crystal orientation on groove stability. So the crystal orientation of the middle grain was required as follows: (i) its (001) crystal plane was oriented in the sample plane (the observation plane); (ii) its ⟨100⟩ crystal axis was tilted by an angle with respect to the temperature-gradient direction to make the left and right grooves asymmetric. Crystal orientations of the neighboring left and right grains were only required to be different from that of the middle grain to form high angle grain boundaries. For the body-centered cubic succinonitrile, its dendrite growing from undercooled melt adopted ⟨100⟩ crystal axe as its preferential growth direction. Thus the dendritic growth morphology can be used to assess the grain orientation. Based on this, the grain selection procedure was as follows. i) The sample was melted and then chilled to nucleate a large number of grains with random orientation. ii) Through careful observation under a microscope, a candidate for the middle grain was searched. It should have four perpendicular primary dendrites in sample plane. The in-plane sidebranches were perpendicular to the dendritic trunk and the vertical constrained sidebranches were located in the midline of the dendrite trunk. When this kind of grain was found, all other grains were melted. iii) The other two grains were produced on the side of the sample cell. Their crystal orientations were very different from that of the middle grain. iv) The selected three grains were controlled to grow epitaxially, and each grain was adjusted to occupy approximate one-third of the sample cell.

A self-designed temperature stage was set up. It consisted of two copper blocks, whose temperatures were controlled by circulating water from two thermostats separately. One copper block was set slightly above the equilibrium melting temperature of sample and the other was below it. When the sample cell was placed in the temperature stage, the solid–liquid interface emerged between two blocks and two GBGs formed at the intersection with grain boundaries. After at least 24-hour annealing at the temperature stage, the morphological stability of GBGs was analyzed with respect to the crystal orientation. Specifically, two sets of experiments were performed. First, one copper was hot, and the other was cold. Two GBGs formed. The left groove of the middle grain was labeled as $L1$, and the right was $R1$. The temperature gradient was denoted by G_1. Then the temperature of copper stage was adjusted. The hot copper was cooled at a slightly lower temperature gradually to freeze the sample. When the sample was solidified entirely, the cold copper was slowly heated at a slightly higher temperature to establish solid–liquid interface again. After equilibrium time, two other GBGs formed. The left groove of the middle grain was denoted as $L2$, and the right marked as $R2$. The temperature gradient was denoted by G_2. The schematic diagram of two sets of experiments is shown in Fig. 1. In two experiments, the sample cell was the same and its position did not change. According to crystallographic symmetry, the grooves at diagonal position have symmetrical orientation. This experimental design can test the effect of crystal orientation on groove stability twice in order to preclude the influence of other experimental disturbances.

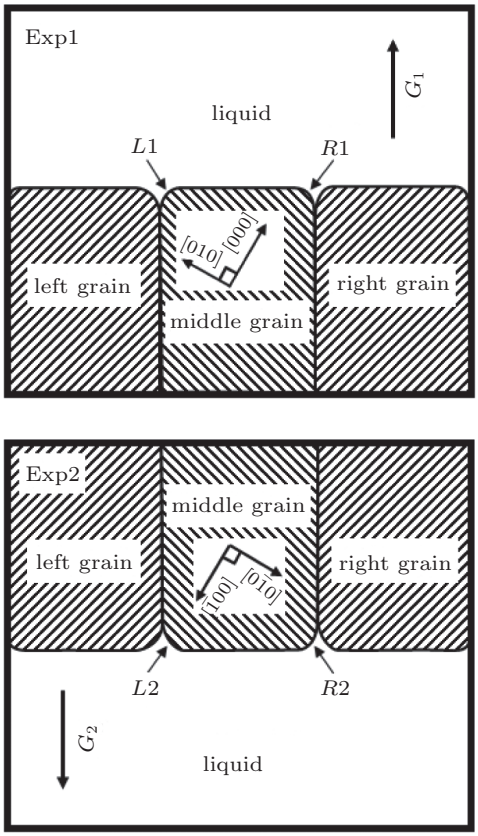


Fig. 1. Schematic diagram of grain boundary grooves with respect to crystal orientations.

The temperature gradient and the interface velocity in our experiment were controlled to be very low. Under these conditions, grooves were large-size and evolved slowly, which was in favor of the observation and identification of their morphological stability with respect to the crystal orientation. The temperature distribution between two blocks was measured with an inserted K-type thermocouple and the temperature gradient at solid–liquid interface was determined.

The morphological evolution of solid–liquid interface was observed and recorded *in situ* with an optical microscopy (Nikon Microphot FXA) and a CCD camera (Olympus DP25). The macroscopic morphology was observed with a 2X objective and GBG morphology was observed with a 40X objective.

The solid–liquid interface was extracted from the recorded images with Canny edge detection algorithm in Matlab. Then, the interface velocity was determined from the interface position with time and the morphological stability of solid–liquid interface was analyzed.

3. Results and discussion

Figure 2 shows the temperature distribution between two copper blocks by a K-type thermocouple inserted in the sample cell. Square symbols denote the temperatures under the first experimental condition, and triangle symbols refer to those under the second experimental condition. Two sets of the measured temperature points are fitted with a quadratic polynomial separately. The crosspoint of two fitted curves indicates the solid–liquid interface position and the equilibrium melting temperature of sample. The derivative of the fitted quadratic polynomials is calculated at solid–liquid interface position and thus the values of G_1 and G_2 are obtained to be 0.341 °C/mm and 0.211 °C/mm respectively. The equilibrium melting temperature is about 55.98 °C. According to the liquidus slope of −3.56 K/wt% in succinonitrile-water alloy, the water content in sample is evaluated to be 0.6 wt% from the equilibrium melting temperature.

The middle grain orientation is assessed from its high-rate dendritic growth morphology as shown by images *O*1 and *O*2 in Fig. 3. It is seen that dendritic stems and sidebranches are perpendicular to each other, which suggests that the (001) crystal plane of the middle grain lies in the sample plane. The dendritic stems are treated as ⟨100⟩ crystal axes, as shown in Fig. 3. The [100] and $[\bar{1}00]$ tilt 29° with respect to the temperature-gradient direction and the [010] and $[0\bar{1}0]$ tilt 61° correspondingly.

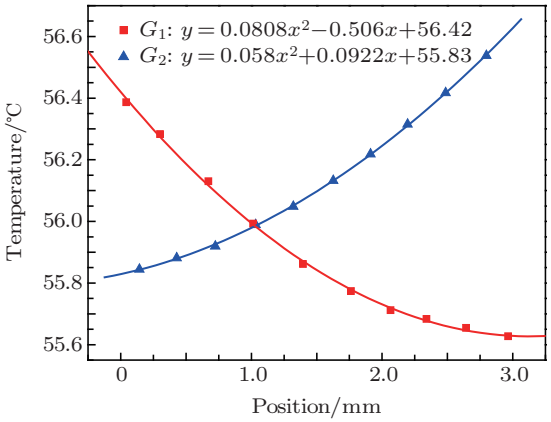


Fig. 2. (color online) Temperature distributions between two copper blocks.

After at least 24-hour annealing under temperature distribution as shown in Fig. 2, the macroscopic solid–liquid interface is observed *in situ* and continuously under low magnification of microscope. It is seen that the macroscopic solid–liquid interface keeps moving back and forth slowly. Through real-time monitor of the interface position, the interface velocity is measured to be less than 0.03 μm/s. The macroscopic interface morphology is planar and keeps stable all the time.

Meanwhile, the morphology evolution of GBGs is also observed and recorded *in situ* under high magnification of microscope. The typical still groove images extracted from the recorded video is shown in Fig. 3. Apparently, the morphologies between the left and right grooves of the middle grain are different under the same temperature gradient. The grooves *L*1 and *R*2 present protrusion and undulation, while the grooves *R*1 and *L*2 have no deformation.

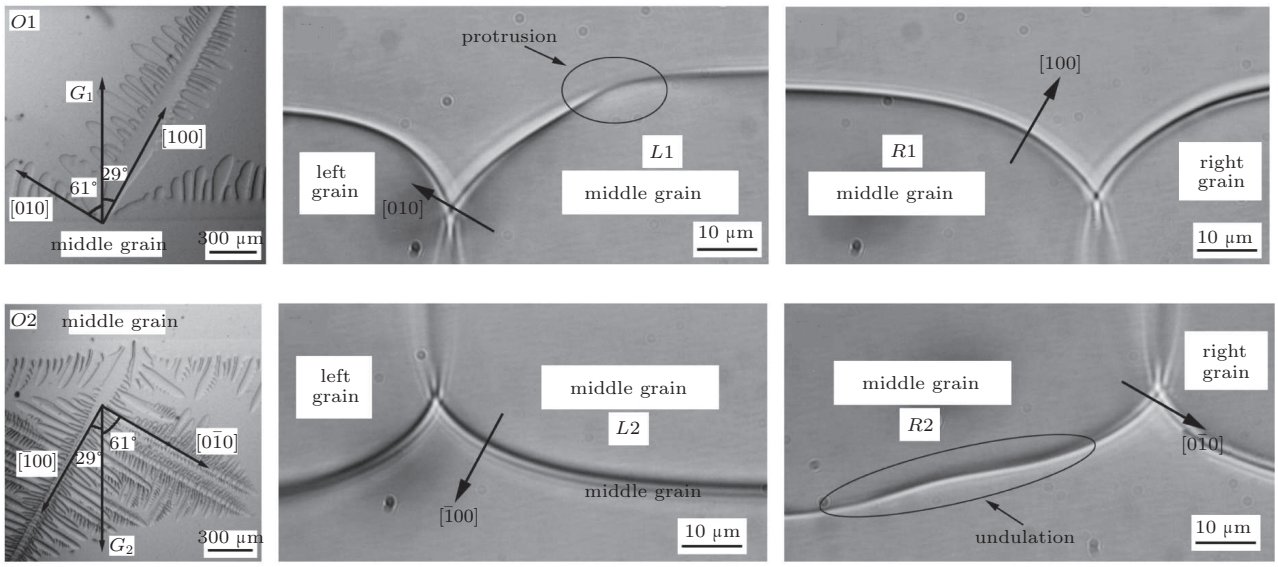


Fig. 3. Dendritic growth morphologies of the middle grain and typical grain boundary grooves at $G_1 = 0.341$ °C/mm (*O*1, *L*1, *R*1) and $G_2 = 0.211$ °C/mm (*O*2, *L*2, *R*2).

For further analysis of the detailed dynamical evolution of these grooves, the groove images at four-minute interval are processed with Canny edge detection algorithm to extract groove morphologies of the middle grain as shown in Fig. 4. The x axis is defined as being along the macroscopic planar solid–liquid interface, and the y axis is defined as being along the temperature-gradient direction from the triple-point of GBG. From Fig. 4, it is seen clearly that grooves $L1$ and $R2$ fluctuate with time while grooves $R1$ and $L2$ keep stable. Regarding the crystal orientation, the grooves $L1$ and $R2$ are at the diagonal position in the (001) crystal plane and thus have symmetrical crystal orientation. So are the grooves $R1$ and $L2$. It can be seen that the groove stability corresponds to the crystal orientation distribution. What is worth mentioning is that the grooves $L1$ and $L2$ are on the left side of the sample with the same grain boundary between the left and the middle grains. And, the grooves $R1$ and $R2$ are on the right side of the sample with the same grain boundary between the right and the middle grains. Apparently, the grooves with a similar morphological stability are not on the same side, but at the diagonal position. This indicates that the different morphological stabilities of grooves under G_1 and G_2 are independent of grain boundary, but relevant to orientation distribution. Specifically, for the stable grooves $R1$ and $L2$, their crystal orientation distributions are around the $\langle 100 \rangle$ crystal axes while for the unstable grooves $L1$ and $R2$, theirs are apart from the $\langle 100 \rangle$ crystal axes. This suggests that the $\langle 100 \rangle$ crystal orientation favors the morphological stability of GBG. Figure 5 shows the interface normal to the grooves $L1$ and $R2$ from one order derivative calculation of their groove shapes, where [010] and $[0\bar{1}0]$ crystal directions are defined as the origin of y axis. It is seen that the grooves $L1$ and $R2$ destabilize in sinusoidal perturbation mode, which is similar to the destabilizing mode of planar interface in directional solidification.

In addition, the macroscopic planar interface under G_1 and G_2 is stable all the time while part of grooves ($L1$ and $R2$) becomes unstable. It means that GBG primarily loses its morphological stability before the instability of the entire planar interface. Meanwhile, it can be seen from Fig. 4 that the deformation amplitude of groove $L1$ under G_1 is smaller than that of groove $R2$ under G_2. This is probably because the temperature gradient G_1 is larger than G_2. That is to say, the temperature gradient is in favor of groove morphological stability.

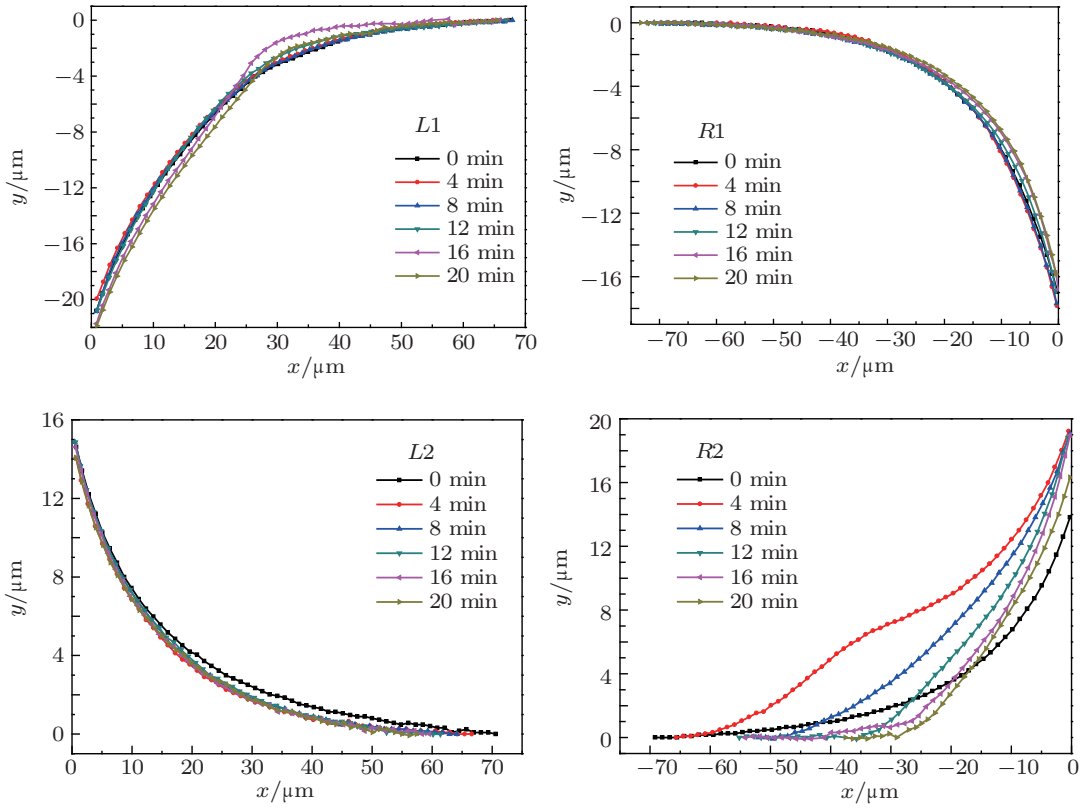


Fig. 4. (color online) Groove shape evolutions of the middle grain at four-minute interval (Each point in plot represents 15 pixels in image).

From the viewpoint of morphology, the relevant stability characteristic of groove with crystal orientation reminds us of the dendritic growth during solidification. Dendrite grows along the $\langle 100 \rangle$ crystal orientation with a stable smooth tip and wave-like branches behind it. So the stable tip is around $\langle 100 \rangle$, while branches initiating behind the tip is apart from

⟨100⟩. Up to now, the questions "why does dendrite adopt preferentially ⟨100⟩ as its growth direction?"[16] and "how do sidebranches form?"[17,18] are still controversial fundamental questions in solidification. The experimental results in this paper imply that the orientation-dependent morphological stability of curved solid–liquid interface may be an intrinsic factor of dendritic pattern formation during solidification.

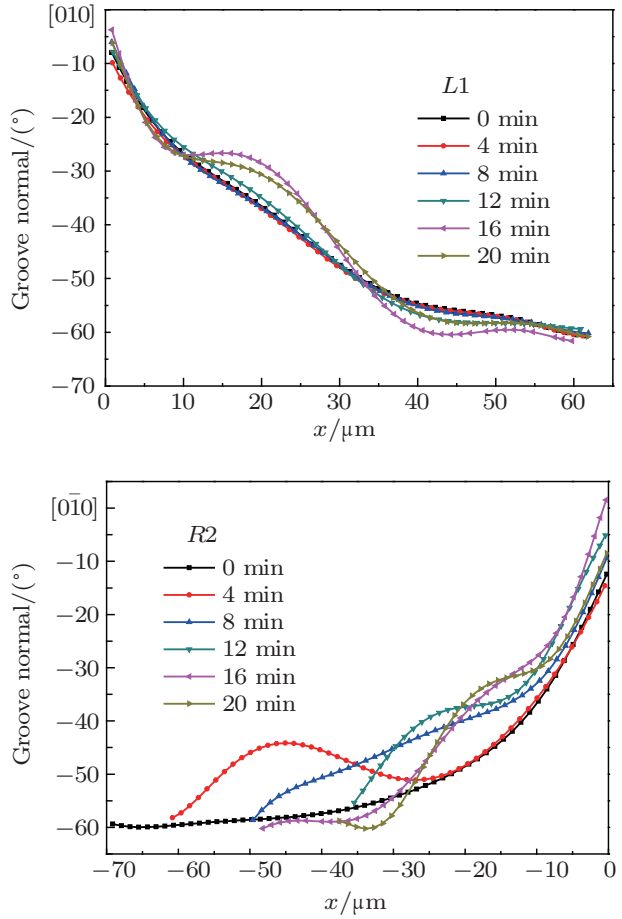


Fig. 5. (color online) Groove normal evolutions of the middle grain at four-minute interval (Each point in plot represents 15 pixels in image).

4. Conclusions

The morphological evolutions near GBGs with different crystal orientations under low temperature gradient and interface velocity are observed in a dilute succinonitrile alloy. Under the experimental conditions, the microscopic solid–liquid interface is planar and keeps stable while part of GBGs becomes unstable. It is found that the morphological stability of GBG is dependent on crystal orientation. Specifically, for succinonitrile with a body-centered cubic structure, GBGs around ⟨100⟩ crystal orientation keep stable while those apart from ⟨100⟩ crystal orientation become unstable under the same conditions. That is to say, ⟨100⟩ crystal orientation favors the morphological stability of GBG.

References

[1] Mullins W W and Sekerka R F 1964 *J. Appl. Phys.* **35** 444
[2] Coriell S R and Sekerka R F 1973 *J. Cryst. Growth* **19** 90
[3] Coriell S R and Sekerya R F 1973 *J. Cryst. Growth* **19** 285
[4] Yeh S Y, Chen C C and Lan C W 2011 *J. Cryst. Growth* **324** 296
[5] Schaefer R J and Glicksman M E 1970 *Metall. Trans.* **1** 1973
[6] Noël N, Jamgotchian H and Billia B 1998 *J. Cryst. Growth* **187** 516
[7] Wang Z J, Wang J C and Yang G C 2008 *Acta Phys. Sin.* **57** 1246 (in Chinese)
[8] Coriell S R and Sekerka R F 1976 *J. Cryst. Growth* **34** 157.
[9] Chen M W, Lan M, Yuan L, Wang Y Y, Wang Z D and Xu J J 2009 *Chin. Phys. B* **18** 1691
[10] Wang Z J, Wang J C and Yang G C 2009 *Phys. Rev. E* **80** 052603
[11] Wang Z J, Wang J C and Yang G C 2010 *Chin. Phys. B* **19** 017305
[12] Wang L L, Wang Z J, Lin X, Wang M and Huang W D 2012 *Chin. Phys. B* **21** 066801
[13] Wang L L, Wang X B, Wang H Y, Lin X and Huang W D 2012 *Acta Phys. Sin.* **61** 148104 (in Chinese)
[14] Wang X B, Lin X, Wang L L, Bai B B, Wang M and Huang W D 2013 *Acta Phys. Sin.* **62** 108103 (in Chinese)
[15] Zhang Y P, Lin X, Wei L, Peng D J, Wang M and Huang W D 2013 *Acta Phys. Sin.* **62** 178105 (in Chinese)
[16] Haxhimali T, Karma A, Gonzales F and Rappaz M 2006 *Nat. Mater.* **5** 660
[17] Glicksman M E, Lowengrub J, Li S and Li X 2007 *Journal of Metals* **59** 27
[18] Muller-krumbhaar H and Langer J S 1981 *Acta Metall.* **29** 145